

A pH-Based Single-Sensor Array for Discriminating Metal Ions in Water

Amy A. Bowyer,^[a] Anthony D. Mai,^[a] Haobo Guo,^[a, b] and Elizabeth J. New^{*[a, c, d]}

Abstract: Human activities, such as mining and manufacturing, expose society and the natural environment to harmful levels of metal ions. Recently, optical sensor arrays for metal ion detection have become popular owing to their favourable features, such as facile sample preparation and the requirement of less expensive instrumentation compared to traditional, spectrometry-based analysis techniques. Sensor arrays usually consist of numerous optical probes that are used in combination to generate unique analyte responses. In contrast, here we present an array that comprises a single

fluorescent sensor, **Coum4-DPA**, that produces unique responses to metal ions in different pH environments. With this simple sensing platform, we were able to classify 10 metal ions in different water sources and quantify Pb^{2+} in tap water using just one fluorescent sensor, a few pH buffers and two sets of spectral data. This novel approach significantly decreases time and costs associated with probe synthesis and data collection, making it highly transferrable to real-world metal sensing applications.

Introduction

In modern times, human industrial activity, such as burning fossil fuels and refining minerals, has amplified the abundance of toxic metals in the environment.^[1] To reduce the harm of metal pollutants, there is a need to not only decrease their production in industrial processes, but also to monitor their occurrence in the environment to minimise contact. Over the past two decades, fluorescent chemosensors have proved to be useful tools for monitoring toxic metals in the environment and biology owing to their high sensitivity and the relative low cost of spectroscopy compared to spectrometry-based methods.^[2] However, many fluorescent chemosensors suffer from a lack of selectivity for a single metal analyte. For example, first row

transition metal ions such as Co^{2+} , Ni^{2+} and Cu^{2+} are notoriously difficult to sense selectively, due to their similar effective ionic radii,^[3] and preferred ligands.^[4]

An alternative strategy to selective sensing is the use of cross-reactive, non-selective probes in a sensor array. Sensor arrays use a combination of sensor elements, or probes, and experimental conditions that generate a unique set of responses for a particular analyte, also known as a fingerprint response.^[5] Multivariate statistical techniques, such as linear discriminant analysis (LDA) or principal component analysis (PCA), make it possible to interpret this fingerprint response and classify similar analytes that would usually not be able to be distinguished by a single fluorescence measurement. Due to the multidimensional nature of the generated data set and machine-learning processes, analytes can be identified without an in-depth understanding of each unique sensor-analyte interaction, making it a “hypothesis-free” analytical technique.

For metal ion sensor arrays reported to date, the most common strategy for achieving diversity is the use of multiple fluorescent probes.^[5a] However, other reported approaches to adding diversity to arrays include collection of optical outputs at different fluorescence/absorbance wavelengths,^[6] applying different stimulus light wavelengths to photo-switchable probes,^[7] different sensor concentrations,^[8] and the use of different solvents.^[9] Another option is to change the pH of the sample solution, as protonating or deprotonating various sensor functional groups can have a significant influence on fluorescence output.^[10] This strategy has been reported in combination with other diversification strategies in arrays for a variety of applications such as identifying lanthanide ions in tap water,^[11] distinguishing various protein populations and human cell lines,^[12] discriminating between ion pairs,^[13] and identifying amino acids.^[14] In these studies, multiple sensors were used alongside a set of pH conditions. However, to the best of our knowledge, pH alone has not yet been employed as the diversification agent in small-molecule sensor arrays for toxic and essential metal ions.

[a] A. A. Bowyer, A. D. Mai, H. Guo, Prof. E. J. New
School of Chemistry
The University of Sydney
Sydney NSW, 2006 (Australia)
E-mail: elizabeth.new@sydney.edu.au

[b] H. Guo
School of Biomedical Engineering
The University of Sydney
Sydney NSW, 2006 (Australia)

[c] Prof. E. J. New
The University of Sydney Nano Institute (Sydney Nano)
The University of Sydney
Sydney NSW, 2006 (Australia)

[d] Prof. E. J. New
Australian Research Council Centre of Excellence for Innovations in Peptide
and Protein Science,
The University of Sydney
Sydney NSW, 2006 (Australia)

Supporting information for this article is available on the WWW under
<https://doi.org/10.1002/asia.202200204>

This manuscript is part of a special collection highlighting Women in Chemistry.

© 2022 The Authors. Chemistry - An Asian Journal published by Wiley-VCH GmbH. This is an open access article under the terms of the Creative Commons Attribution Non-Commercial License, which permits use, distribution and reproduction in any medium, provided the original work is properly cited and is not used for commercial purposes.

By using this single-sensor array approach, we can significantly decrease time and costs associated with synthesising and analysing numerous probes, while retaining high classification accuracy. We chose pH as the diversification agent in our single-sensor array because pH buffers are inexpensive, widely-available, safe to handle, effective in low concentrations and they eliminate the need to add large quantities of organic solvent to the sample.

Here we report the use of a fluorescent coumarin sensor, **Coum4-DPA**, as a single sensor element in an array to discriminate between biologically-essential and toxic metal ions. We use the fluorescence intensity responses of **Coum4-DPA** to the metal ions in various pH conditions and the statistical method, LDA, to predict group membership and to discriminate between the metal ions (Figure 1). A highlight of this single-sensor pH array is that it is non-responsive and therefore robust to high levels of commonly-occurring cations such as Ca^{2+} and Mg^{2+} . As a result, the array was successfully applied to analyse a variety of sample environments including tap water and dam water.

Results and Discussion

Small molecule sensors that are capable of producing a wide range of fluorescence responses to different analytes are highly useful in sensor arrays. We identified **Coum4-DPA** as an “always-on” probe that can experience both increases and decreases in fluorescence intensity in response to stimuli. **Coum4-DPA** is a 7-hydroxy-4-methylcoumarin with a dipicolyl-amine (DPA) metal-chelating group at the 8-position (Figure 2a). The hydroxyl group functions as the internal charge transfer (ICT) donor, while the DPA group partially quenches the fluorescence of the coumarin fluorophore *via* a photoinduced electron transfer (PET) mechanism, evidenced by the lower fluorescence intensity of **Coum4-DPA** compared to Coumarin 4 (Figure S1). In this way, both pH fluctuations and metals ions can interfere with the hydroxyl group to quench fluorescence *via* inhibited ICT, whereas any interaction of analytes at the DPA

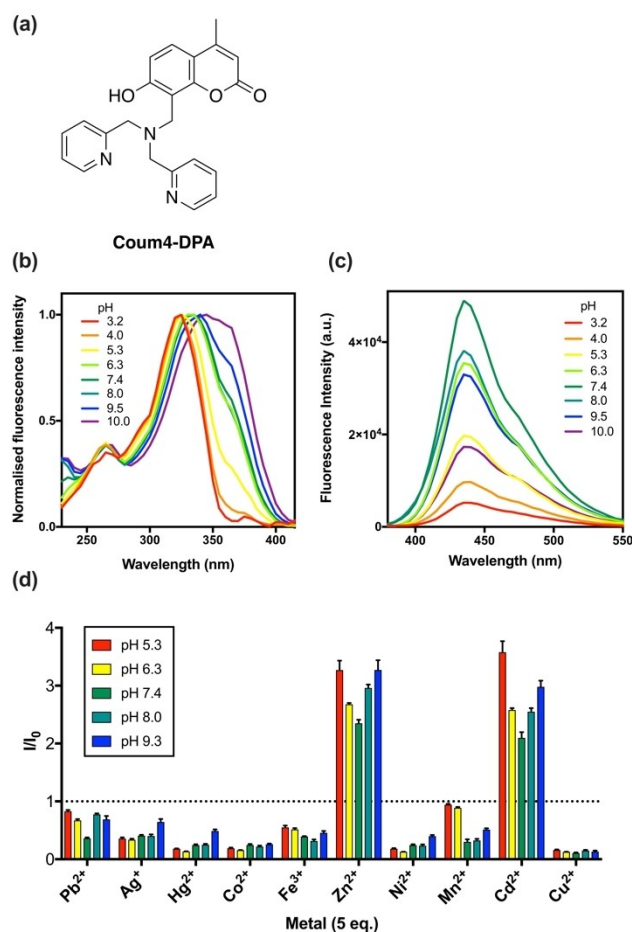


Figure 2. (a) Structure of **Coum4-DPA**. (b) Normalised excitation ($\lambda_{em} = 435$ nm) spectra of **Coum4-DPA** (10 μM) in buffered Milli-Q water (20 mM buffer). (c) Emission ($\lambda_{ex} = 335$ nm) spectra of **Coum4-DPA** (10 μM) in buffered Milli-Q water (20 mM buffer). (d) Normalised fluorescence emission responses of **Coum4-DPA** (10 μM) to metal ions (50 μM) in 1:99 DMF/pH buffer (20 mM) $\lambda_{ex} = 335$ nm, $\lambda_{em} = 355$ –600 nm. Error bars represent standard deviation, n = 5.

group could decrease PET and enhance fluorescence (Scheme S1).

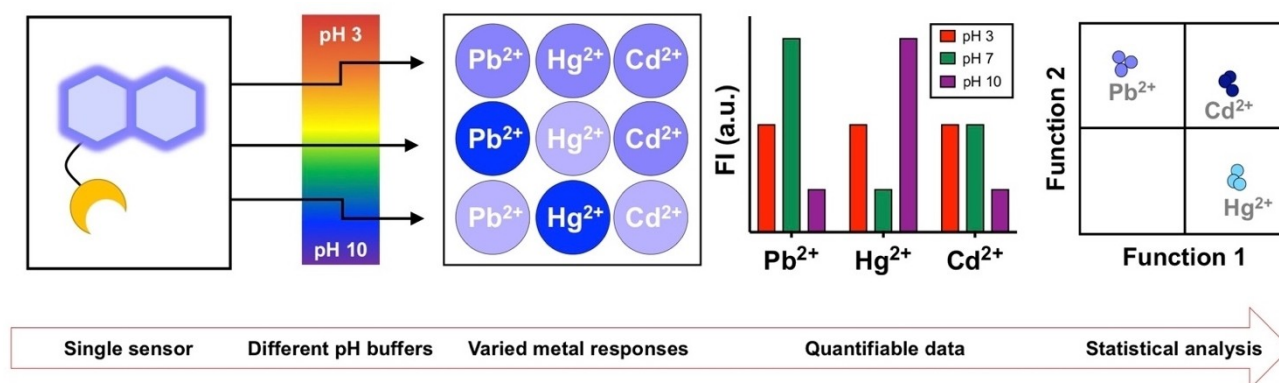


Figure 1. A schematic representation of a single-sensor array using pH environment as a diversification agent for the discrimination of metal ions. Pb^{2+} , Hg^{2+} and Cd^{2+} are given as example analytes and pH 3, 7 and 10 are given as example pH buffer variables.

We first synthesised and used **Coum4-DPA** as a sensor element in a three-sensor array for heavy metals previously reported by our research group.^[15] It was synthesised in a single step from commercially-available starting materials, 7-hydroxy-4-methylcoumarin (Coumarin 4) and 2,2'-dipicolylamine.^[15] The excitation maximum of **Coum4-DPA** shifts from 325–365 nm with increasing pH from 3.2 to 10.0 (Figure 2b), due to the deprotonation of the hydroxy group in basic conditions, $pK_a = 9.4$ (Figure S2). Regardless of pH, the emission maximum remains at 435 nm, although intensity varies, with neutral pH values aligning with highest fluorescence output (Figure 2c, photophysical summary provided in Table S1).

Fluorescence responses of **Coum4-DPA** to metal ions varied. Most metal ions quenched the fluorescence intensity of **Coum4-DPA**; some metals, such as Zn^{2+} and Cd^{2+} , enhanced the fluorescence intensity (Figure 2d), while highly-abundant group I and II metal ions had minimal influence on fluorescence and cannot be distinguished from a blank sample (Figure S3). We speculate that fluorescence turn-on responses occur when the metal ion, such as Zn^{2+} , binds to the DPA receptor group, lessening the PET quenching of the DPA group (Figure S1). Alternatively, it is likely that quench responses result when the metal ion binds directly to the hydroxyl group of **Coum4-DPA**, reducing ICT efficiency, decreasing fluorescence. These turn-on/off responses of hydroxy-coumarins have been suggested by Kobayashi *et al.* in their solvent-dependent metal sensor.^[16]

Encouragingly, the five buffered pH environments clearly changed the fluorescence response of individual metal ions, generating several different fingerprint responses. Some metals, such as Ag^+ , Hg^{2+} and Ni^{2+} displayed an increasing trend in normalised fluorescence with pH, while other metal ions, such as Pb^{2+} , Fe^{3+} , Zn^{2+} , Mn^{2+} and Cd^{2+} displayed higher normalised fluorescence values at lower pH environments, a trough in intensity at neutral pH, then an increase at higher pH values (Figure 2d). The fluorescence response of a single metal ion varies across pH buffers because fluctuations in the concentration of hydrogen ions in the analysis environment change the ability of metal ions to interact with the heteroatoms responsible for influencing the fluorescence output of **Coum4-DPA**.

With some promising, well-resolved fingerprint responses across the five pH buffers tested, we proceeded with array-based sensing of 10 metal ions including: toxic metal ions, Pb^{2+} , Ag^+ , Hg^{2+} and Cd^{2+} ; and essential transition metal ions, Co^{2+} , Fe^{3+} , Zn^{2+} , Ni^{2+} , Mn^{2+} and Cu^{2+} . The fluorescence emission spectra of **Coum4-DPA** in the presence of metal ions were collected, integrated and normalised against the fluorescence of **Coum4-DPA** alone. LDA was performed on five replicate normalised fluorescence responses of **Coum4-DPA** to 10 metal ions. The first two generated discriminant functions contributed to 99.7% of the variance, while the three remaining functions were less useful in discriminating between metal ions (Figure 3a, for 95% confidence ellipses see Figure S4). The analysis was able to correctly classify 100% of the metal ions with five pH buffers. Leave-one-out cross validation was 98% accurate, with only one Hg^{2+} sample being incorrectly classified as Ni^{2+} in this more robust test (Table S2).

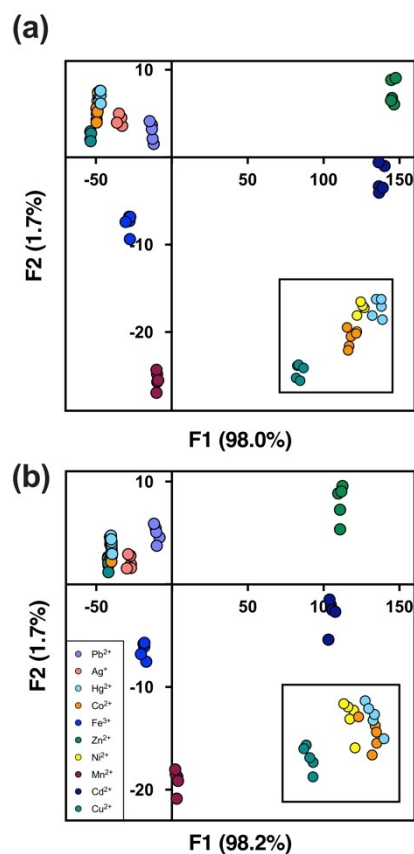


Figure 3. LDA score plots for the analysis of 10 metal ions (50 μ M metal ion, 10 μ M **Coum4-DPA** ($\lambda_{ex} = 335$ nm, $\lambda_{em} = 355$ –600 nm)) in buffered Milli-Q water (20 mM, pH 5.3–9.5), and DMF (1% (v/v)), $n = 5$: a) using five pH buffers (5.3, 6.3, 7.4, 8.0, 9.5); and b) using three pH buffers (pH 6.3, 8.0, 9.5). Insets: magnifications of the Hg^{2+} , Co^{2+} , Ni^{2+} and Cu^{2+} clusters.

Reducing the number of sensor elements or assay conditions in an array significantly decreases the time and costs of identifying metal ions. In a single-sensor array such as this, the only way to simplify the array is to decrease the number of pH conditions. Upon interpretation of the metal fingerprint responses to five buffers (Figure 2d), it is visible that for most metals, buffered environments at pH 5.3 and 6.3 produced very similar normalised fluorescence responses of **Coum4-DPA**. This is to be expected, considering that the pK_a of **Coum4-DPA** is 9.4, resulting in similar ratios of protonated and deprotonated species at these low pH values. As a result, pH 5.3 was omitted from the array.

Furthermore, most metal ions also produced similar results at pH 7.4 and pH 8.0 for the same reasons. Owing to this, pH 7.4 was also omitted from the array. LDA of the resulting three-buffer array (pH 6.3, 8.0 and 9.5) classified metal ions with 100% and 98% accuracies for the original test and the cross-validation test respectively (Table S3), despite visible clustering of metals ions such as Hg^{2+} , Co^{2+} , Ni^{2+} and Cu^{2+} (Figure 3b, for 95% confidence ellipses see Figure S4). To further validate the success of the three-buffer array, data was also analysed by a support vector machine with Gaussian kernel. The confusion matrix output gave 100% correct predictions of 10 metals

(Table S4) and the 2D projection of the classifiers on the data set shows good division between 10 metal analytes, as well as division from Ca^{2+} and Mg^{2+} interferants (Figure S5).

In addition to the 100% accuracy of the three-buffer array, another notable feature is that commonly occurring metal ions, such as Ca^{2+} and Mg^{2+} , have a minimal impact on the fluorescence **Coum4-DPA** (Figure S3) compared to essential transition metals and toxic metals. This creates the possibility for the array to function in other environments where Ca^{2+} and Mg^{2+} levels are naturally high, such as tap water. Prior to tap water testing, the three-buffer array was trialled in Milli-Q water spiked with low and high levels of Ca^{2+} and Mg^{2+} to replicate soft and hard water respectively. The array performed well in these initial tests, with LDA classifying all 10 metal ions correctly with 100% accuracy in the initial analysis and the leave-one-out cross-validation test (Tables S5 & S6). Furthermore, visualisation of both LDA score plots showed excellent separation of Ca^{2+} and Mg^{2+} from essential and toxic metals (Figure S6). This ensures that high levels of Ca^{2+} and Mg^{2+} will not produce a false positive result for the presence of other metal ions.

To further test the robustness of the single-sensor array system, the analysis was conducted in a tap water sample. Inductively-coupled plasma mass spectrometry (ICP-MS) and anion chromatographic analysis was performed to determine inherent levels of metal ions and common anions respectively (Tables S7 & S8). The total hardness of the tap water sample was determined to be 13.1 ppm, and it can therefore be classified as soft water under Australian and WHO drinking water guidelines.^[17] The tap water was then spiked with 10 metal ions and subjected to array analysis. For tap water analysis we did not add any organic solvent to the sensing matrix in order to better replicate real-world testing conditions. Initial analysis in three pH buffers (6.3, 8.0 and 9.5) gave 90% correct classification, dropping to 76% accuracy with cross-validation (Figure 4a, Table S9). Errors included misclassifying Ag^+ as Fe^{3+} and Hg^{2+} as Ni^{2+} . The array did not perform as well in tap water because the metal analyte fingerprint responses to **Coum4-DPA** were less distinguishable than in the Milli-Q water analysis (Figure S7). This is likely because the pre-existing chemical and biological components of tap water may interfere with the ability of the metal ions to interact with **Coum4-DPA**. Unsurprisingly, the tap water had significant, high micromolar concentrations of Na^+ , Ca^{2+} and Cl^- (Tables S7 and S8). Furthermore, inherent levels of Cu^{2+} in the tap water sample will also interact with **Coum4-DPA**, dampening the response of **Coum4-DPA** to the metal analyte in the discrimination analysis.

A common strategy for increasing the discrimination power of a sensor array is to include more spectroscopic data in the analysis. We had previously observed that the excitation maximum of **Coum4-DPA** undergoes a red shift with increasing pH (Figure 2b). By collecting two emission spectra ($\lambda_{\text{ex}} = 335 \text{ nm}$, $\lambda_{\text{em}} = 355\text{--}600 \text{ nm}$ and $\lambda_{\text{ex}} = 355 \text{ nm}$, $\lambda_{\text{em}} = 375\text{--}600 \text{ nm}$) of tap water buffered at pH 6.3, 8.0 and 9.5, we obtained a six-variable dataset without any extra sample preparation. LDA of this six-variable data set led to 100% correct classification of all 10 essential and toxic metals (Table S10). However, the more robust, leave-one-out cross-validation test dropped to 92%

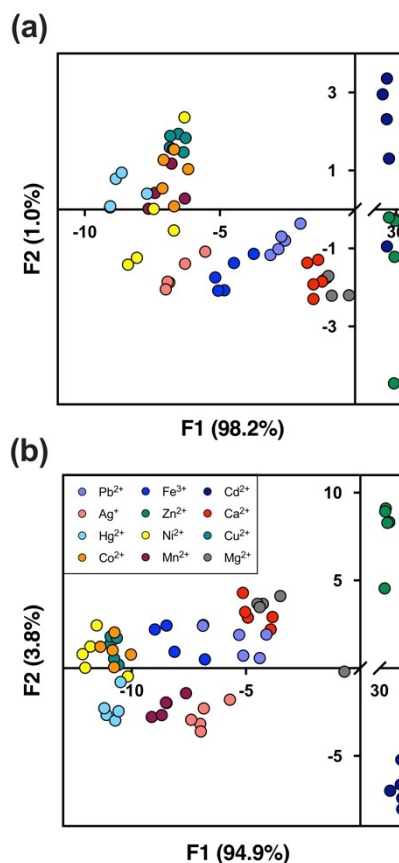


Figure 4. LDA score plots for the analysis of 10 metal ions ($50 \mu\text{M}$ metal ion, $10 \mu\text{M}$ **Coum4-DPA**) in buffered tap water (20 mM , pH 6.3, 8.0, 9.5) without organic solvent, $n = 5$: a) using a single spectrum analysis ($\lambda_{\text{ex}} = 335 \text{ nm}$, $\lambda_{\text{em}} = 355\text{--}600 \text{ nm}$); and b) using double spectrum analysis ($\lambda_{\text{ex}} = 335 \text{ nm}$, $\lambda_{\text{em}} = 355\text{--}600 \text{ nm}$, $\lambda_{\text{ex}} = 355 \text{ nm}$, $\lambda_{\text{em}} = 375\text{--}600 \text{ nm}$).

(Table S10). The first three discriminant functions contributed 94.9%, 3.8% and 0.8% of the variance respectively. Plotting the metal scores of these functions against each other shows good resolution of some metal ions like Zn^{2+} and Cd^{2+} (Figure 4b, for 95% confidence ellipses see Figure S8). However, other metals that typically generate a fluorescence quenching response to **Coum4-DPA** were less well-resolved visually on the LDA score plot in tap water compared to the more controlled analysis matrices. This is not surprising because tap water is a complex mixture containing a variety of biological and chemical components that can interfere with the sensing ability of the array. Fortunately, a second application of LDA for only the metal ions in this cluster (Hg^{2+} , Co^{2+} , Ni^{2+} and Cu^{2+}) produces excellent discrimination (Figure S9, Table S11), and we were nevertheless pleased by the marked improvement in discriminating power achieved simply by using an additional excitation wavelength.

The three-pH array was also successfully applied to discriminate 10 metal ions in an environmental, dam water sample. LDA correctly classified five replicates of each metal ion with 100% accuracy in both the initial analysis and the leave-one-out cross-validation test (Figure S10, Table S12). Unlike tap water

analysis, this sample did not require data from the additional excitation wavelength to obtain 100% accuracy.

We have, so far, been able to demonstrate that the three-buffer pH array scaffold using **Coum4-DPA** is a useful tool for distinguishing harmful metals, such as Pb^{2+} and Cd^{2+} , from essential metal ions. As a result, we decided to test the ability of our array platform to quantify Pb^{2+} in tap water. Pb^{2+} was chosen as the example analyte owing to the real possibility of Pb^{2+} exposure from tap water, such as the occurrence of the Flint Water Crisis in Michigan, United States.^[18] In these experiments, eight different micromolar concentrations of Pb^{2+} were analysed with LDA, which achieved a high classification accuracy of 88.8%. This value only dropped slightly to 87.5% upon cross-validation (Table S13). Visualisation of the LDA score plot of this analysis shows good clustering of each concentration group (Figure 5a). The only misclassifications made by the array were of neighbouring concentrations, such as 100 μM samples being misclassified as 120 μM (Table S13). Furthermore, when five test samples containing 85 μM Pb^{2+} were added to the analysis as unknowns, they were all classified as 70 μM , the closest training concentration available (Figure 5a, Table S13). In this way, the three-buffer array can be used as a semi-quantitative method for Pb^{2+} detection.

While determining approximate concentrations of Pb^{2+} with LDA is a useful and valid technique, using a machine-learning regression analysis technique allows for more precise unknown concentrations to be resolved. The three-buffer training data from the semi-quantitative Pb^{2+} array was modelled using the Gaussian Process Regression (GPR) method, giving an excellent fit of actual *versus* predicted concentrations (Figure 5b). When tested with the GPR model, test concentrations of 85 μM gave an average prediction of 83.2 ± 3.6 μM (standard deviation, $n = 5$), demonstrating that the array is able to act as an accurate quantification tool when used in this way. Notably, when the same regression analysis was repeated with fewer pH buffers, the model was less successful at predicting trained data, as well as the unknown test cases (Figure S11), highlighting the utility of a cross-reactive array approach for quantifying toxic metals in tap water.

Conclusion

In summary, we have devised a robust sensor array for the identification of essential and toxic metal ions using a single, fluorescent probe, **Coum4-DPA**. The sensor, **Coum4-DPA**, satisfies the criteria of a single sensor element in a pH-based array. It is synthetically-accessible, being prepared through a simple, single-step synthetic procedure and is water soluble, forgoing the need of including large proportions of organic solvents in the analysis mixture. It is an ideal probe for sensor arrays because it produces a variety of turn-on and turn-off fluorescence emission intensity responses across all 10 metal analytes. Furthermore, it is inherently pH-sensitive, shifting fluorescence spectral windows in different pH conditions. This enables more data to be collected, thus adding more variation into the array without additional sample preparation.

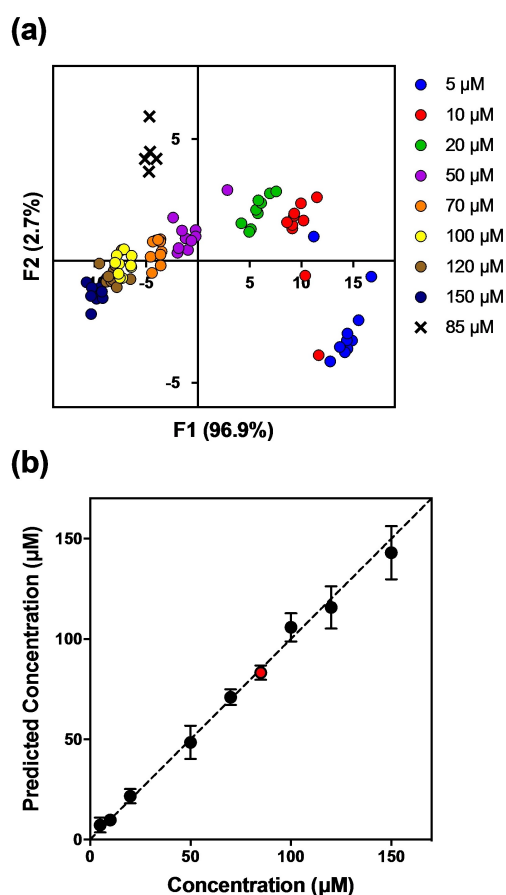


Figure 5. Semi-quantitative and quantitative analysis of Pb^{2+} in tap water. (a) LDA score plot for the semi-quantitative analysis of Pb^{2+} with (10 μM **Coum4-DPA**) in buffered tap water (20 mM, pH 6.3, 8.0, 9.5) (no DMF) using a single integrated fluorescence measurement ($\lambda_{\text{ex}} = 335$ nm, $\lambda_{\text{em}} 355\text{--}600$ nm). Circles are training data used in the LDA ($n = 10$), crosses are test data ($n = 5$), entered as unknowns in the analysis and assigned function scores. (b) Plot of predicted vs. actual concentrations Pb^{2+} given by GPR analysis (rational quadratic kernel) of the three-buffer array (pH 6.3, pH 8.0, pH 9.5, 20 mM) in tap water (no DMF) using a single integrated fluorescence measurement ($\lambda_{\text{ex}} = 335$ nm, $\lambda_{\text{em}} 355\text{--}600$ nm) for train (black) and test (red) data. $y = x$ is plotted for reference, the regression produced root mean squared error and R-squared values of 8.02 and 0.98 respectively. Error bars represent the standard deviation of ten (black) or five (red) replicate samples, error bars were not drawn where the standard deviation was less than the length of the symbol.

Initial arrays in Milli-Q water only required three variables (three different pH buffers) in order to discriminate 10 metal ions. This is a promising result for environmental applications of sensor arrays; saving time and costs associated with statistical analysis. Furthermore, the limited response of **Coum4-DPA** to Ca^{2+} and Mg^{2+} allows for the single-sensor array system to be used in a wide variety of analysis media, such as tap water samples. The three-buffer sensor array achieved 100% correct classification in both artificial soft and hard water samples, as well as a real tap water sample. This is important for potential applications of this system, as the water quality, including water hardness, can vary greatly within a single city. Finally, the three-buffer array proved a useful tool for quantifying toxic Pb^{2+} , which could accurately be measured in tap water samples with machine-learning regression analysis.

Experimental Section

Coum4-DPA was synthesised according to previously-published procedures.^[15]

Data collection for array-based sensing

All array data was collected on a PerkinElmer EnSpire Multimode Plate Reader in 300 μL , 96-well polypropylene microplates (Item No.: 655209, greiner Bio-One). Samples were prepared by mixing aqueous metal salt stock solutions (2 mM) and freshly-prepared aqueous **Coum4-DPA** stock solution (2 mM) in pH buffers (20 mM). The final concentrations of **Coum4-DPA** and metal ions were 10 μM and 50 μM respectively for qualitative analysis and 10 μM and 5 μM –150 μM respectively for quantitative metal analysis. Buffers for analysis (20 mM) were prepared by diluting aqueous buffer stocks (100 mM) in one of five water sources: Milli-Q water, artificial soft water, artificial hard water, tap water (Camperdown, Sydney, Australia) and water collected from Manly Dam, Sydney, Australia. A buffer concentration of 20 mM was chosen based on a buffer capacity experiment that demonstrated sufficient pH-buffering at 20 mM (Figure S12). Arrays in Milli-Q, artificial soft and artificial hard water also contained 1% (v/v) DMF to aid the solubility of **Coum4-DPA**. No DMF or other organic solvent was added to any tap water or dam water samples. For each buffer replicate, a control well containing no metal ion was included to normalise the data prior to statistical analysis. The microplate was shaken for 5 s and incubated at 25 °C for 1 h. A 1 h incubation time was selected to ensure adequate mixing and signal stabilisation before data was collected (Figure S13). Each well was excited at 335 nm and fluorescence emission spectra were collected from 355–600 nm at 5 nm increments. An additional data set was collected by exciting at 355 nm and collecting the fluorescence emission spectra from 375–600 nm at 5 nm increments for qualitative tap water data analysis only. For all qualitative array analysis the experimental design consisted of five replicates of each unique metal/buffer combination (1 sensor \times 3(5) pH buffers \times 10 metal ions \times 5 repetition per analyte = 1 \times 3(5) \times 10 \times 5 data points = 150(250) data points); for tap water analysis only, an additional variable of emission spectrum was added (1 sensor \times 3 pH buffers \times 2 spectral windows \times 10 metal ions \times 5 repetition per analyte = 1 \times 3 \times 2 \times 10 \times 5 data points = 300 data points) For quantitative analysis, ten replicates of each unique concentration/buffer combination was used for the training set (1 sensor \times 3 pH buffers \times 1 spectral window \times 8 Pb^{2+} concentrations \times 10 repetition per concentration = 1 \times 3 \times 1 \times 8 \times 10 data points = 240 data points) and five replicates were used for the test set (1 sensor \times 3 pH buffers \times 1 spectral window \times 1 Pb^{2+} concentration \times 5 repetition per concentration = 1 \times 3 \times 1 \times 1 \times 5 data points = 15 data points).

Data handling and statistical analysis

All data for qualitative analysis were analysed in SPSS Statistics version 26 (IBM). Normalised integrated emission spectra were subjected to linear discriminant analysis (LDA) in which the metal analytes were input as the grouping variable and normalised sensor responses as independent variables. The data were classified as all groups being equal. Combined groups plots and classification with leave-one-out cross-validation summary tables were produced for interpretation. Discriminant scores and predicted membership were also recorded. For unknown sample classification, data was excluded from the grouping variable and LDA was used to predict group membership by assigning discriminant function values for each replicate and assigning them a location on the territorial map. A second method of metal classification was performed on the three-buffer, 10 metal data set in Milli-Q water using the

classification learner app in MATLAB R2019b, training for all support vector machine (SVM) models. An SVM model with a fine Gaussian kernel was selected, as it had the highest accuracy (100%). Pb^{2+} quantification regression analysis was performed in MATLAB R2019b, using the regression learner app, training for all regression models. A Gaussian Process Regression (rational quadratic) was the chosen regression model as it had the lowest root mean squared error for the Pb^{2+} concentration training data.

Analysis matrix preparation

According to the World Health Organisation (WHO), total water hardness below 60 mg/L is soft; between 60–120 mg/L is moderately hard; between 120–180 mg/L is hard; and above 180 mg/L is very hard.^[17a] Artificial soft and hard water samples were prepared by dissolving quantitative masses of calcium nitrate tetrahydrate and magnesium nitrate hexahydrate in Milli-Q water (1 L). Total hardness (in CaCO_3 equivalents) calculations were performed on all water samples used in array analysis (Section 1.2).

Tap and dam water analysis

Metal concentrations in tap water and dam water were determined by ICP-MS in triplicate (PerkinElmer Nexion 300X) with instrument specifications outlined in the in supporting information (Table S14). Anion concentrations in tap water were analysed by ion chromatography (Dionex ICS 1000). Water samples were centrifuged (4000 rpm, 10 minutes) and filtered through nylon 0.22 μm membrane filters prior to ICP-MS and anion chromatography analysis.

Acknowledgements

The authors would like to acknowledge the Australian Research Council (DP180101353), Westpac Scholars Trust for a Research Fellowship (EJN), the University of Sydney for a SOAR Fellowship (EJN), the Australian government for a Research Training Program Scholarship (AAB), the Henry Bertie and Florence Mabel Gritton Medallist Award (AAB), and the Australian Research Council Training Centre for Innovative BioEngineering for PhD support (HG). We thank Dr Nicholas Proschogo for ICP-MS analysis. Open access publishing facilitated by The University of Sydney, as part of the Wiley - The University of Sydney agreement via the Council of Australian University Librarians.

Conflict of Interest

The authors declare no conflict of interest.

Data Availability Statement

The data that support the findings of this study are available from the corresponding author upon reasonable request.

Keywords: fluorescence spectroscopy · heavy metals · sensor array · sensors · transition metals

- [1] M. C. Navarro, C. Pérez-Sirvent, M. J. Martínez-Sánchez, J. Vidal, P. J. Tovar, J. Bech, *J. Geochem. Explor.* **2008**, *96*, 183–193.
- [2] a) E. J. New, *ACS Sens.* **2016**, *1*, 328–333; b) T. Rasheed, M. Bilal, F. Nabeel, H. M. N. Iqbal, C. L. Li, Y. F. Zhou, *Sci. Total Environ.* **2018**, *615*, 476–485; c) H. N. Kim, W. X. Ren, J. S. Kim, J. Yoon, *Chem. Soc. Rev.* **2012**, *41*, 3210–3244; d) D. Wu, A. C. Sedgwick, T. Gunnlaugsson, E. U. Akkaya, J. Yoon, T. D. James, *Chem. Soc. Rev.* **2017**, *46*, 7105–7123; e) G. Chen, Z. Guo, G. Zeng, L. Tang, *Analyst* **2015**, *140*, 5400–5443; f) M. Dutta, D. Das, *TrAC Trends Anal. Chem.* **2012**, *32*, 113–132.
- [3] R. D. Shannon, *Acta Crystallogr. Sect. A* **1976**, *32*, 751–767.
- [4] R. G. Pearson, *J. Chem. Educ.* **1968**, *45*, 581–587.
- [5] a) D. Smith, I. Topolnicki, V. Zwicker, K. Jolliffe, *Analyst* **2017**, *142*; b) Z. Li, J. R. Askim, K. S. Suslick, *Chem. Rev.* **2019**, *119*, 231–292; c) P. J. Anzenbacher, P. Lubal, P. Buček, M. A. Palacios, M. E. Kozelkova, *Chem. Soc. Rev.* **2010**, *39*, 3954–3979.
- [6] a) A. Kapf, M. Albrecht, *J. Mater. Chem. B* **2018**, *6*, 6599–6606; b) A. M. Mallet, Y. Liu, M. Bonizzoni, *Chem. Commun.* **2014**, *50*, 5003–5006; c) J. Du, Y. Deng, Y. He, *Analyst* **2019**, *144*, 5420–5424; d) Q. Wang, Q. Liu, X.-M. Du, B. Zhao, Y. Li, W.-J. Ruan, *J. Mater. Chem. C* **2020**, *8*, 1433–1439.
- [7] M. S. Hossain, S. A. Rahaman, J. Hatai, M. Saha, S. Bandyopadhyay, *Chem. Commun.* **2020**, *56*, 4172–4175.
- [8] H. Li, M. Jiā, J. R. Askim, Y. Zhang, C. Duan, Y. Guan, L. Feng, *Chem. Commun.* **2014**, *50*, 15389–15392.
- [9] D. G. Smith, L. Mitchell, E. J. New, *Analyst* **2019**, *144*, 230–236.
- [10] a) A. P. De Silva, H. N. Gunaratne, T. Gunnlaugsson, A. J. Huxley, C. P. McCoy, J. T. Rademacher, T. E. Rice, *Chem. Rev.* **1997**, *97*, 1515–1566; b) J. Yin, Y. Hu, J. Yoon, *Chem. Soc. Rev.* **2015**, *44*, 4619–4644.
- [11] B. Roy, T. S. Roy, S. A. Rahaman, K. Das, S. Bandyopadhyay, *ACS Sens.* **2018**, *3*, 2166–2174.
- [12] a) S. Tomita, S. Ishihara, R. Kurita, *ACS Appl. Mater. Interfaces* **2017**, *9*, 22970–22976; b) H. Sugai, S. Tomita, S. Ishihara, R. Kurita, *ACS Sens.* **2019**, *4*, 827–831.
- [13] Y.-I. Liu, M. A. Palacios, P. Anzenbacher, *Chem. Commun.* **2010**, *46*, 1860–1862.
- [14] F. Zaubitzer, A. Buryak, K. Severin, *Chem. Eur. J.* **2006**, *12*, 3928–3934.
- [15] A. A. Bowyer, C. Shen, E. J. New, *Analyst* **2020**, *145*, 1195–1201.
- [16] H. Kobayashi, K. Katano, T. Hashimoto, T. Hayashita, *Anal. Sci.* **2014**, *30*, 1045–1050.
- [17] a) World Health Organization, WHO Press, Geneva, Switzerland, **2011**;
b) National Health and Medical Research Council, National Resource Management Ministerial Council, *Australian Drinking Water Guidelines Paper 6 National Water Quality Management Strategy, Vol. 3.5*, Commonwealth of Australia, Canberra, **2011**.
- [18] K. J. Pieper, M. Tang, M. A. Edwards, *Environ. Sci. Technol.* **2017**, *51*, 2007–2014.

Manuscript received: March 2, 2022
Revised manuscript received: March 24, 2022
Version of record online: April 7, 2022